Computer Methods and Programs in Biomedicine 260 (2025) 108520

Contents lists available at ScienceDirect

Computer Methods and Programs in Biomedicine

journal homepage: www.sciencedirect.com/journal/computer-methods-and-programs-in-biomedicine

A model-based quantification of nonlinear expiratory resistance in Plethysmographic data of COPD patients

Theodore Lerios [a,*], Jennifer L. Knopp [a], Camilla Zilianti [b], Matteo Pecchiari [c], J. Geoffrey Chase [a]

[a] Department of Mechanical Engineering, Centre for Bio-Engineering, University of Canterbury, Christchurch, New Zealand
[b] Dipartimento di Scienze Biomediche e Cliniche Luigi Sacco, Universit`a degli Studi di Milano, Milan, Italy
[c] Dipartimento di Fisiopatologia Medico-Chirurgica e dei Trapianti, Universit`a degli Studi di Milano, Milan, Italy

ARTICLE INFO

Keywords:
Plethysmographic loops
Airway resistance
Chronic obstructive pulmonary disease
Respiratory function tests
Respiratory pathophysiology
Respiratory mechanics
Respiratory modelling

ABSTRACT

Background: Chronic obstructive pulmonary disease (COPD) is characterised by airway obstruction with an increase in airway resistance (R) to airflow in the lungs. An extreme case of expiratory airway resistance is expiratory flow limitation, a common feature of severe COPD. Current analyses quantify expiratory R with linear model-based methods, which do not capture non-linearity's noted in COPD literature. This analysis utilises a simple nonlinear model to describe patient-specific nonlinear expiratory resistance dynamics typical of COPD and assesses its ability to both fit measured data and also to discriminate between severity levels of COPD.

Methods: Plethysmographic data, including alveolar pressure and airway flow, was collected from n=100 subjects (40 healthy, 60 COPD) in a previous study. Healthy cohorts included Young (20–32 years) and Elderly (64–85 years) patients. COPD patients were divided into those with expiratory flow limitation (FL) and those without (NFL). Inspiratory R was treated as linear ($R_{1,insp}$). Expiratory R was modelled with two separate models for a comparison: linear with constant resistance ($R_{1,exp}$), and nonlinear time-varying resistance ($R_{2,exp}(t)$) using b-splines.

Results: Model fit to PQ loops show inspiration is typically linear. Linear $R_{1,exp}$ captured expiratory dynamics in healthy cohorts (RMSE 0.3 [0.2 - 0.4] cmH_2O), but did not capture nonlinearity in COPD patients. COPD cohorts showed PQ-loop ballooning during expiration, which was better captured by non-linear $R_{2,exp}(t)$ (RMSE 1.7 [1.3–2.8] vs. 0.3[0.2–0.4] cmH_2O in FL patients). Airway resistance is higher in COPD than healthy cohorts (mean $R_{2,exp}(t)$ for Young (1.9 [1.6–2.8]), Elderly (2.4 [1.4–3.5]), NFL (4.9 [3.9–6.6]) and FL (13.5 [10.4–21.9]) $cmH_2O/L/s$, with $p \leq 0.0001$ between aggregated measures for Young and Elderly healthy subjects and NFL and FL COPD subjects). FL patients showed non-linear $R_{2,exp}(t)$ dynamics during flow deceleration, differentiating them from NFL COPD patients.

Conclusions: Linear model metrics describe expiration dynamics well in healthy subjects, but fail to capture nonlinear dynamics in COPD patients. Overall, the model-based method presented shows promise in detecting expiratory flow limitation, as well as describing different dynamics in healthy, COPD, and FL COPD patients. This method may thus be clinically useful in the diagnosis or monitoring of COPD patients using Plethysmography data, without the need for additional expiratory flow limitation confirmation procedures.

1. Introduction

Chronic obstructive pulmonary disease (COPD) describes a collection of chronic inflammatory lung diseases, and is a common cause of death and disability globally [1,2]. COPD is also one of the most common reasons for intensive care unit (ICU) admission [2]. COPD is estimated to cost the United States upward of $72 billion (~ 0.35 % of GDP) per annum [3] in direct costs alone, but is often overlooked by governments, healthcare systems, and the pharmaceutical industry [4]. Recent studies show 3.2 million deaths per year were due to COPD, and COPD is the 7th leading cause of years of life lost [5].

Although COPD is is strongly related to tobacco smoking, its underlying causes are more widespread. Factors increasing COPD risk include a history of respiratory infection, including HIV or tuberculosis,

* Corresponding author.
E-mail addresses: leriosted@gmail.com (T. Lerios), Geoff.Chase@canterbury.ac.nz (J.G. Chase).

https://doi.org/10.1016/j.cmpb.2024.108520
Received 27 May 2024; Received in revised form 30 September 2024; Accepted 16 November 2024
Available online 30 November 2024

and exposure to dust, indoor pollution, or chemical agents and fumes [1, 6–8]. Respiratory illness is classified by restrictive and obstructive lung function, where restrictive diseases affect both inflow and outflow, and obstructive diseases primarily affect exhalation. Pulmonary function is commonly assessed with spirometry or full body plethysmography [9].

Airway obstruction is observable as an increased resistance to airflow in the lungs [10]. While healthy subjects airway resistance increases slightly with age [11], it rises markedly in COPD subjects, especially during expiration [12–16]. An extreme case of expiratory flow resistance is expiratory flow limitation (EFL), where a maximum flow exists such that an increased pressure gradient cannot achieve higher flow [17]. When EFL occurs not only during a forced expiration, but also during tidal breathing, tidal EFL (tEFL) is present. EFL is a well defined mechanical-pathophysiological condition in COPD subjects at rest or during exercise [16–19]. EFL is a major determinant of exercise limitation in COPD [12], since patients with EFL exhibit decreased inspiratory capacity (IC) throughout exercise [13,20]. Bronchodilation is a common treatment, but its use in COPD patients is affected by the presence and severity of EFL [21–26].

Subjects presenting with tEFL often have more advanced COPD, but EFL can be difficult to diagnose, requiring the negative expiratory pressure (NEP) technique or surrogate techniques, such as forced oscillations or plethysmography [17]. During NEP, negative pressure is applied at the mouth during tidal expiration, and the resulting flow volume loop is compared with the previous measured control loop [14]. There is no current standardised method for NEP loop interpretation, relying instead on investigator experience [25].

Spirometry is commonly performed in patients with respiratory diseases. Plethysmography can provide added information, such as total lung capacity (TLC), and functional residual capacity (FRC) [27]. In comparison, Plethysmography provides added information, such as total lung capacity (TLC) and functional residual capacity (FRC) [27]. Breathing manoeuvres are used to asses whether a patient has reduced airflow or lung capacity, indicating possible respiratory disease. However, results are highly dependent on the patient's ability to cooperate correctly and participate in the test [28]. Use of NEP, or other tEFL detection methods [26], require further additional procedures, specialist equipment, patient-cooperation during breathing manoeuvres, and/or clinical expertise for result interpretation [26,29]. Overall, it is thus difficult to diagnose or assess, limiting diagnosis and monitoring of response to care overtime.

Model-based, non-invasive, patient-specific methods can identify pulmonary mechanics and dynamics where other invasive methods fail [30–35]. They have potential to capture varying disease states within COPD pathology from easily measured airway pressure and flow during tidal breathing. Previous model-based approaches have assumed resistance changes linearly with flow. However, in contrast, clinical and physiological literature show strong non-linearity in expiratory resistance with respect to flow [27,29,36–38]. Other clinical analyses have attempted to quantify disease state using the shape or area of the pressure-flow or pressure-volume loop [29,36].

This analysis combines the linear approach and a new nonlinear expiratory resistance model to capture the nonlinear, patient-specific expiratory resistance dynamics typical of COPD. There is thus a new nonlinear modeling approach taken to capture those dynamics not captured by linear resistance. Plethysmographic data obtained from previous studies [29,39] is used to validate a model-based approach based on both model fit to measured data, as well as ability to potentially discriminate between clinically assessed COPD severity levels. In particular, the nonlinearity of expiratory resistance in healthy young subjects, healthy elderly patients, non-flow-limited COPD patients (NFL) and flow-limited COPD patients (FL) is explored to assess a potential model-based diagnostic and metric based on commonly acquired Plethysmographic data, where healthy individuals would be expected to have minimal nonlinearity beyond the linear expiratory resistance expected, NFL patients moderate to more severe nonlinearity, and FL patients the most nonlinearity captured by the new nonlinear expiratory resistance model term. This outcome is important as a model-based method for diagnosis, which did not require FVC or similar maneuver, could enable easier diagnosis and reduce misdiagnosis of those less able to perform these maneuvers.

2. Methods

2.1. Clinical data

Plethysmographic data from 100 subjects, including 40 healthy subjects and 60 COPD patients, was collected in previous studies [29,39] focused on COPD and pulmonary function testing [29,36]. Full study methodology and details can be found in [29,36], describing 4 cohorts: 20 Young (20–32 years) and 20 Elderly (64–85 years) healthy subjects, and 60 COPD patients (age > 50 years), 25 with no expiratory flow limitation (NFL) and 35 patients with expiratory flow limitation (FL). Flow limitation was assessed by the NEP method [17], where a -5 cmH_2O pressure was applied at the mouth during quiet breathing, and flow-volume (Q-V) loops of control and applied NEP breaths were compared. Standard FVC tests were also performed, as shown in Table 1, and show the expected decreasing trend with age, COPD status, and flow limitation. Patient demographics can be found in Table 1. Both healthy cohorts were confirmed to have no flow limitation via NEP.

Plethysmographic data was collected using a constant volume Plethysmograph (MasterScreen Body Plethysmograph, Erich Jaeger GmbH,Wurzburg, Germany) and includes alveolar pressure ($P_{alv}(t)$) and flow at the airway opening ($Q(t)$). Intrathoracic gas volume (ITGV) was measured near end-expiration during quiet breathing. [29,36]. P_{alv} is derived from changes in barometric pressure inside the plethysmography box using Boyle's law [27] and shift volume. Data from COPD patients includes plethymographic measurements from before bronchodilator administration. Long- and short- acting bronchodilators were withdrawn 24 and 8 hours before the study, respectively [29].

2.2. Model-based analysis

2.2.1. Linear single compartment model

Pressure drop across the airways is typically defined as a function of flow rate:

$$P_{aw}(t) - P_{alv}(t) = RQ(t) \tag{1}$$

Where $P_{aw}(t)$ [cmH_2O] is airway pressure, $Q(t)$ [L/s] is airflow, and R [$cmH_2O/L/s$] is airway resistance. In current standard analyses, R is assumed constant with time. In plethysmography, P_{alv} is calculated relative to the atmospheric pressure [29,36], which also represents the pressure at the airway opening. Thus, Eq. 1 reduces to:

$$-P_{alv}(t) = RQ(t) \tag{2}$$

Airway resistance is known to differ between inspiration and

Table 1
Demographic data is median [Inter-quartile range] where relevant. FRC = functional residual capacity; VT = tidal volume; VC = vital capacity TLC = Total lung capacity; FVC = forced vital capacity; ITGV = intra-thoracic gas volume.

	Young	Elderly	NFL	FL
# Subjects	20	20	25	35
M/F	13/7	17/3	15/10	22/13
AGE (years)	22 [21–24]	71 [69–72]	71 [67–74]	72 [69–78]
BMI	23 [20–25]	26 [24–28]	27 [24–29]	25 [23–27]
FRC (L)	3.3 [2.6–3.9]	3.5 [3.2–4.3]	4.0 [3.3–4.5]	5.0 [4.2–5.9]
VT (L)	0.8 [0.3–1.3]	0.7 [0.3–1.1]	0.9 [0.4–1.5]	0.7 [0.3–1.1]
VC (L)	5.4 [4.1–5.9]	4.1 [3.5–4.8]	2.4 [3.0–3.7]	1.8 [2.3–3.1]
TLC (L)	7.3 [5.8–8.2]	6.7 [6.0–8.0]	6.4 [5.7–8.0]	7.3 [5.8–8.1]
FVC (L)	5.3 [5.0–5.9]	3.8 [3.4–4.5]	2.4 [1.9–3.1]	1.7[1.4–2.2]
ITGV (L)	3.5 [2.7–4.1]	3.5 [3.0–4.1]	4.0 [3.3–4.6]	5.0[4.2–6.0]

expiration [40,41]. Thus, airway resistance is identified separately for inspiration and expiration, yielding $R_{1,insp}$ and $R_{1,exp}$.

$$-P_{alv}(t) = \begin{pmatrix} R_{1,insp}Q(t) & t_{insp} \\ R_{1,exp}Q(t) & t_{exp} \end{pmatrix} \tag{3}$$

Model identification is carried out in Matlab (The Mathworks, Inc., Natick, Massachusetts, United States.) using its built in linear least squares function 'lsqlin', which constrains all identified parameters positive, which is physiologically realistic [42]. This linear model formulation still holds resistance constant over the inspiratory and expiratory periods. It thus may not fully capture airway dynamics in COPD patients, where expiratory resistance can be volume dependent and nonlinear [12,27,29,36,37].

2.2.2. Nonlinear single compartment model

It is hypothesised a non-linear resistance is required to capture the non-linear airway behaviour during expiration in flow limited patients, which is critical to diagnosis and further monitoring. The non-linear resistive model incorporates the constant linear term ($R_{1,insp}$) identified during inspiration (Q_{insp}) alongside an additional dynamic resistive term ($R_{2,exp}(t)$), during expiration. Thus, Eq. 3 becomes:

$$-P_{alv}(t) = \begin{pmatrix} R_{1,insp}Q(t) & t_{insp} \\ R_{2,exp}(t)Q(t) & t_{exp} \end{pmatrix} \tag{4}$$

$R_{2,exp}(t)$ is modelled using a summation of M 2nd order ($d = 2$) b-spline functions ($\Phi_1(t)$: $\Phi_M(t)$) to fit the unknown shape function, capturing any non-linear, time-varying dynamics during expiration:

$$R_{2,exp}(t) = \sum_{i=1}^{M} a_i \Phi_{i,d=2}(t)$$

$$-P_{alv}(t) = \begin{pmatrix} R_{1,insp}Q(t) & t_{insp} \\ \left[\sum_{i=1}^{M} a_i \Phi_{i,d=2}(t)\right] Q_{exp}(t) & t_{exp} \end{pmatrix} \tag{5}$$

Where a_i are constant coefficients of the splines ($\Phi_i(t)$) identified using the linear least squares method from plethysmographic data. The second order b-splines are defined over time [33,43–45]:

$$\Phi_{i,0}(t) = \begin{pmatrix} 1 & T_i \le t \le T_{i+1} \\ 0 & otherwise \end{pmatrix}$$

$$\Phi_{i,d}(t) = \frac{t - T_i}{T_{i+d} - T_i}\Phi_{i,d-1}(t) + \frac{T_{i+d+1} - t}{T_{i+d+1} - T_{i+1}}\Phi_{i+1,d-1}(t) \quad for \quad d \ge 1 \tag{6}$$

The number (M) of 2nd order ($d = 2$) splines with knots (T_i) of width k_w=0.01s and time span T_{max} = expiratory duration is defined:

$$M(n) = ceil\left(\frac{T_{max}(n)}{k_w}\right) + d \tag{7}$$

Linear least squares is again used for model identification of $R_{1,insp}$ to identify the a_i coefficients of $R_{2,exp}(t) = \sum a_i \Phi_i(t)$ using the regression equation defined:

$$\begin{bmatrix} Q_{insp} & \varnothing & \dots & \varnothing \\ \varnothing & \Phi_1, Q_{exp} & \dots & \Phi_M Q_{exp} \end{bmatrix} \begin{bmatrix} a_1 \\ a_2 \\ \vdots \\ a_M \end{bmatrix} = [-P_{alv}] \tag{8}$$

2.2.3. Analyses

The identified parameters and model fit of the linear model of (Eq. 3) are compared to those of the nonlinear model of (Eq. 5), where the $R_{1,exp}$ constant changes to a nonlinear, time-varying $R_{2,exp}(t)$. Both models are fit to the plethysmographic pressure and flow data over expiration to yield expiratory resistances $R_{1,exp}$ and $R_{2,exp}(t) = {}^{P}(a_i\Phi_i)$, respectively, for each subject. $R_{1,exp}$ and $R_{2,exp}(t)$ are expected to be similar for healthy subjects, as both terms are capturing the same linear, constant parameter dynamics. However, larger values of mean $R_{2,exp}(t)$ are expected for NFL and FL COPD subjects with their expected, clinically observed larger and nonlinear expiratory resistance. In both cases, inspiration is modelled with a linear resistance, $R_{1,insp}$. Model fit is assessed via root mean squared error (RMSE).

Inspiratory and expiratory resistance are compared, and expected to be strongly linearly related with $R_{1,exp} > R_{1,insp}$ [40]. PQ loops are presented, as they are used clinically to evaluate COPD [12,29,36,37,39]. Where inspiratory and expiratory resistance is purely linear, the PQ loop reduces to two straight lines with slopes of R_{insp} and R_{exp} respectively. As non-linearity in airway resistance increases, one or both halves of the PQ loop balloons out.

The shape of $R_{2,exp}(t)$) with time and flow is assessed to examine the time and potential flow dependence of airway resistance during expiration, where previous clinical work suggests a flow or volume dependent resistance [6,24,41]. The following metrics are used to assess nonlinear resistance differences between cohorts: 1) Mean non-linear expiratory resistance: mean($R_{2,exp}(t)$) =mean(${}^{P}(R_2\Phi)$); and 2) Area under the QR curve: $AUC_{RQ} = {}^{R}_{exp}\, QdR$. The student's t-test is used where relevant to assess likely statistically significant differences between comparators ($p \le 0.05$), thus assessing diagnostic potential metrics across sub-cohorts.

3. Results

PQ loops with clinical data and model-fit to data in Fig. 1 show linear resistance models are acceptable across inspiration and expiration for healthy Young and Elderly cohorts. In contrast, the FL COPD patient is not well captured by the linear model, and significant expiatory dynamics are missed. In particular, the expiratory looping is completely missed by the linear model in Fig. 1.

As a result, model error in Table 2 increases with COPD for the linear model, and is significantly higher ($p \le 0.0001$) in the FL cohorts. This outcome for the linear model indicates significant limitations on the use of this model in FL COPD patients, as well as for some NFL subjects. Expiratory resistance values in Table 2 are higher than inspiratory resistance, irrespective of whether the model is linear ($R^2 = 0.85$) or non-linear ($R^2 = 0.70$), as expected. Equally, these results match the FVC values for these cohorts in Table 1, where the more severe the COPD, the lower the FVC, again, as expected. Thus, the results for $R_{2,exp}(t)$ the nonlinear resistance term capture a measure of the progression of COPD, particularly in delineating FL from NFL and healthy cohorts, supporting the FVC values found in Table 1 in the original experimental study.

Fig. 2 shows $R_{2,exp}(t)$ increases nonlinearly over expiration in COPD cohorts, particularly in FL cohorts. Plotting non-linear $R_{2,exp}(t)$ against flow shows the non-linear dynamics mostly occur during decelerating exhalatory flow, particularly towards the end of the breath. This behaviour matches expected patterns for end-expiratory flow limitation [29,37,39]. Typical patients are shown alongside patients with the highest and lowest mean $R_{2,exp}(t)$ from each cohort. Fig. 3 shows while $R_{2,exp}(t)$ can overlap in magnitude between FL patients and NFL patients with very high airway resistance, the dynamic shape is different. In particular, the NFL subject with high $R_{2,exp}(t)$ exhibits significant nonlinearity across all expiratory flow, in contrast to the predominantly decelerating flow dynamic of FL patients. One Elderly patient (outlier) appears to show resistance dynamics more typical of FL patients.

Healthy patients have overlapping $R_{1,insp}$ ([1.3 [1.1 - 1.6] vs. 1.8 [1.2 - 2.2] $cmH_2O/L/s$, $p = 0.04$) and $R_{1,exp}$ resistance (1.8 [1.2 - 2.2] vs. 2.4 [1.5 - 2.9] $cmH_2O/L/s$, $p = 0.62$) outcomes across the Young and Elderly cohorts, with airway resistance slightly higher, on average, in the Elderly cohort. Resistance is higher in COPD cohorts (mean $R_{2,exp} = 2.1$ [1.5 - 3.1] vs. 10.3 [5.4 - 16.2] $cmH_2O/L/s$, $p \le 0.0001$, for healthy and COPD cohorts respectively), with $meanR_{2,exp}$ most pronounced in the FL cohort in Fig. 3 (mean $R_{2,exp}$ = 13.5 [10.4–21.9] vs. 2.1 [1.5 - 3.1] $cmH_2O/L/s$ in healthy subjects, $p \le 0.0001$). Cohort overlap in resistance

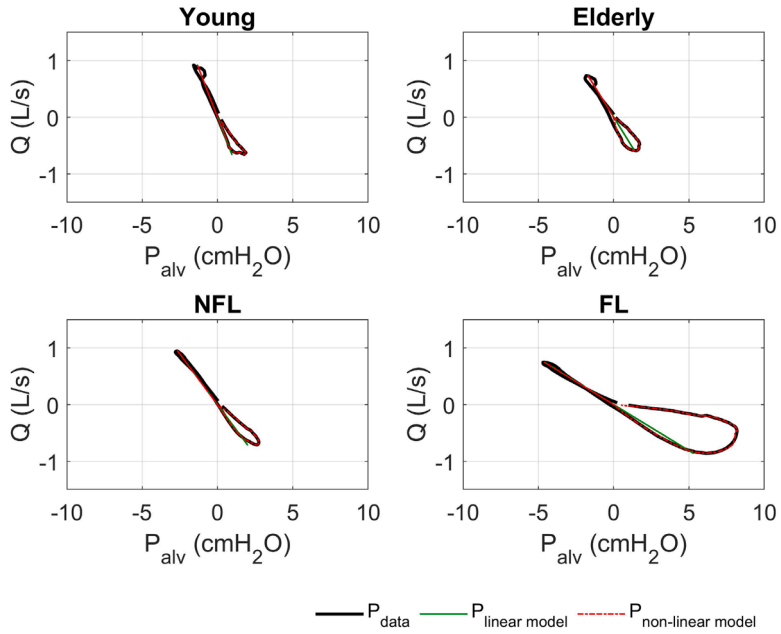

Fig. 1. PQ loops for alveolar pressure (P_{alv}) with the linear and nonlinear model fits. The linear model only shows every 10th data point for clarity and ease of reading the plot. The results show the clear growth of an expiratory loop and loss of slope in the PQ plot as COPD presents and becomes more severe for FL cases.

Table 2
Median [IQR] of model parameters and fit error for linear and nonlinear models for the Young (Y), Elderly (ELD), and COPD subjects (NFL and FL).

		Linear		Nonlinear	
	$R1,insp$ [$cmH_2O/L/s$]	$R_{1,exp}$ [$cmH_2O/L/s$]	RMSE [cmH_2O]	Mean $R_{2,exp}(t)$ [$cmH_2O/L/s$]	RMSE [cmH_2O]
Y	1.3 [1.1–1.6]	1.7 [1.5–2.8]	0.3 [0.2–0.3]	1.9 [1.6–2.8]	0.1 [0.1–0.1]
ELD	1.8 [1.2–2.2]	2.4 [1.5–2.9]	0.3 [0.3–0.4]	2.4 [1.4–3.5]	0.1 [0.1–0.1]
NFL	3.0 [2.7–3.6]	4.2 [3.7–6.6]	0.6 [0.4–1.0]	4.9 [3.9–6.6]	0.1 [0.1–0.2]
FL	5.9 [4.6–7.9]	5.9 [8.6–15.4]	1.7 [1.3–2.8]	13.5 [10.4–21.9]	0.3 [0.2–0.4]

values in Fig. 3 demonstrates resistance values ($R_{1,insp}$, mean$R_{2,exp}$) alone are insufficient as a clinical marker to accurately distinguish patients with COPD and/or tEFL, despite FL and NFL cohorts having statistically different mean $R_{2,exp}$ ($p \leq 0.0001$) values.

Fig. 4 shows AUC-RQ is more effective at distinguishing between COPD patients with and without FL ($p \leq 0.0001$), although some overlap remains. Fig. 1 suggests these overlapping NFL patients with high AUC-RQ can be visually differentiated by the shape of the **PQ** plot. In particular, by the size of the balloon or loop evident in FL subjects in comparison with NFL subjects, as well as the change in slope seen, both as shown in Fig. 1 and in starker comparison to healthy young and elderly subjects.

Fig. 4 shows strong linearity and inter-cohort consistency between the young and old healthy subjects and even the NFL subjects when comparing $R_{1,exp}$ and mean $R_{2,exp}$ ($R^2 = 0.85$). However, many FL subjects show a divergence from this linear best fit trend, indicating nonlinear dynamics in expiration are most apparent in this cohort, matching Fig. 2 and as expected, clinically. Thus, overall, NFL patients show higher airway resistance than young and elderly otherwise healthy cohorts, and FL patients are distinguishable by their significantly nonlinear expiratory resistance.

4. Discussion

This study presents a model-based method for examining nonlinear expiratory resistance in COPD patients using standard spirometry PQ loops. The novel finding in this analysis is COPD patients with FL can be distinguished from healthy and NFL COPD cohorts by their significant nonlinearly increasing airway resistance at end-expiration, particularly during decelerating flow. This outcome matches and objectively quantifies previous work [29] analysing PQ loop ballooning in patients with tEFL, providing additional descriptive metrics enabling identification of patients with tEFL via Plethysmographic data alone.

The results presented here indicate limitations in the relatively common use of linear, or averaged, airway resistance models, an assumption underlying most clinical literature in this area to date [12,15,25,29,36–39,46–48]. Appendix A includes an example of a patient's plethysmographic data (Fig. 5; Appendix A), and every result for each patient is shown in Table 3, including identified model parameters for every patient in each respective cohort. Such models show good model-fit to data in healthy subjects, and may even be reasonably reflective of underlying airway dynamics in some NFL COPD patients, as shown in Figs. 1, 2 and Table 2. In contrast, FL COPD patients had significant PQ loop ballooning, not captured by the linear model, particularly during decelerating flow. Previous work [29] has captured these PQ loop abnormalities via geometric metrics, such as PV loop areas (work of resistance) combined with peak flow. This study adds to previous work through quantification of time and flow-varying effective airway resistance over expiration, and does so within a model-based framework used in respiratory digital twins [30,49,50].

By definition, tEFL indicates a decoupling of flow from applied airway pressure gradients, with flow limited to some maximum value. This behaviour is reflected in the non-linear resistance as sharply increasing resistance, denoting greater pressure gradient per unit flow.

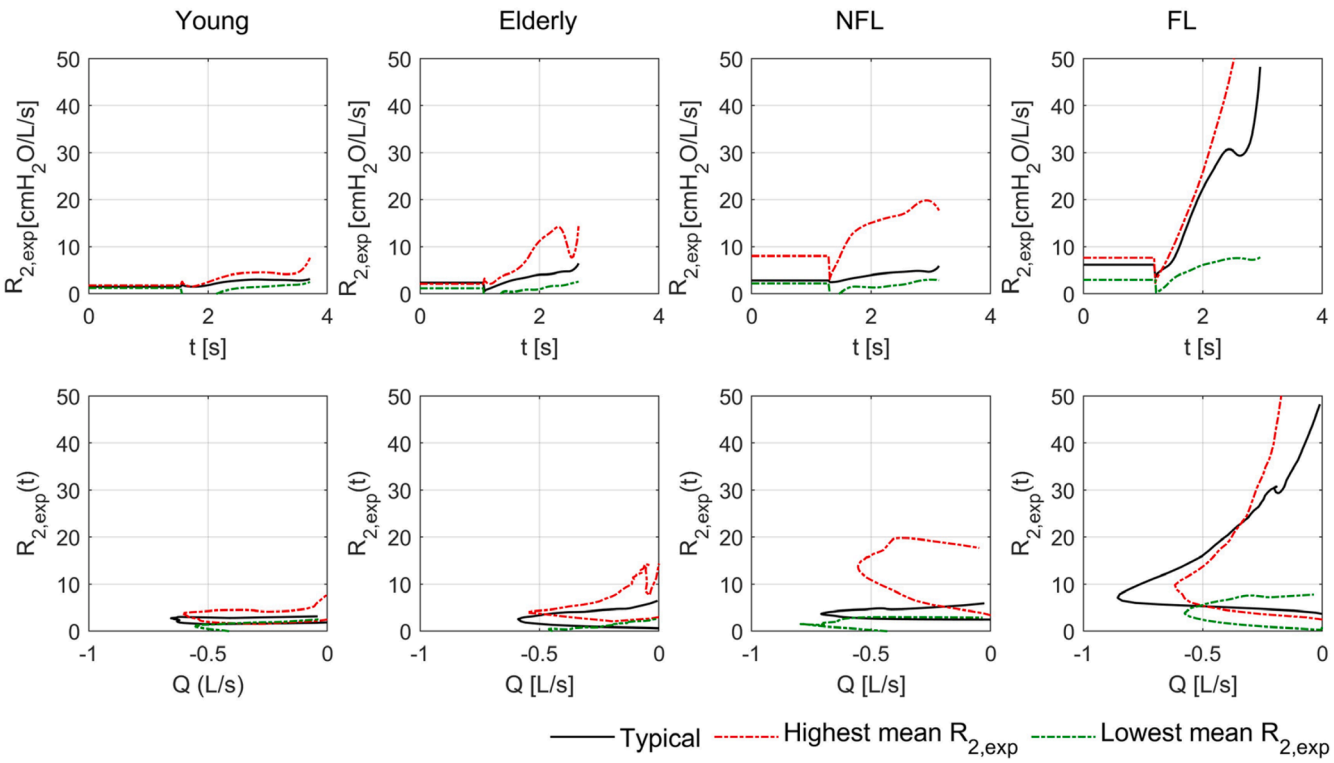

Fig. 2. Time (top) and flow-course (bottom) of nonlinear expiratory resistance ($R_{2,exp}$) for three example patients from each cohort.

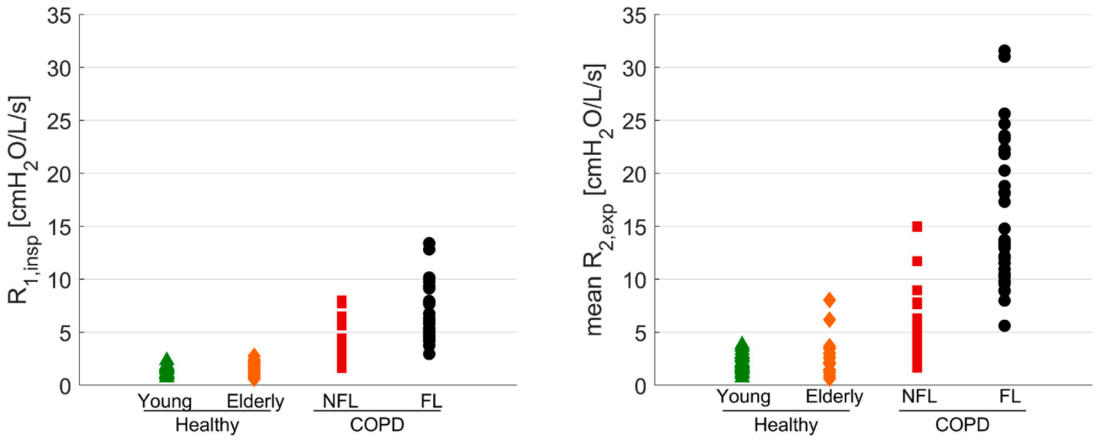

Fig. 3. Inspiratory and mean non-linear expiratory resistance $R_{2,exp}$ for all four patient cohorts.

This nonlinearity is greatest during decelerating flow, as shown in Fig. 2. Such behaviour during decelerating flow was not apparent in NFL COPD subjects, even those with high expiratory resistance. Nonlinearity in the Elderly subjects with the highest expiratory resistance, such as the outlier in Fig. 4, suggests this patient may be beginning to experience COPD-like dynamics. Overall, Fig. 4 shows FL COPD patients can be distinguished from healthy patients with high specificity.

NFL COPD patients can be thought of as an 'intermediate' disease stage in the healthy to severe progression, with higher resistance compared to healthy subjects and different expiatory resistance shape dynamics compared to either healthy or FL COPD subjects. Thus, model-based nonlinear expiratory resistance derived from plethysmographic data may be a clinically useful tool in the diagnosis and monitoring of COPD progression. This outcome results from the ability of models to better quantify dynamics which might be less directly apparent in the data.

Several mechanisms contribute toward the progression of EFL by reducing the expiratory flow reserve in the tidal volume range [18]. Increased airway resistance, age, obesity, augmented cholinergic bronchial tone, decreased lung elastance, airway- parenchyma uncoupling, and airways collapsibility are all mechanisms of EFL [18]. Predominant reduction of maximal expiratory flow rates at lower lung volumes appears more crucial in promoting EFL [18]. In the presence of EFL, deformation of airways at choke points and downstream segments, coupled with local high air velocity, and possibly with small airways collapse, may cause peripheral airway and parenchymal injury [20].

Pecchiari et al [29] suggest tEFL contributes significantly to PQ loop ballooning in COPD, adding to other mechanisms, such as lung heterogeneity, air trapping, and lung recruitment [29]. They show highly correlated ($R_2 = 0.8$))inspiratory and expiatory PV loop area under the curve (AUC-PV) in NFL patients, where AUC-PV corresponds work of resistance, since the PV loops in this case utilise relative alveolar

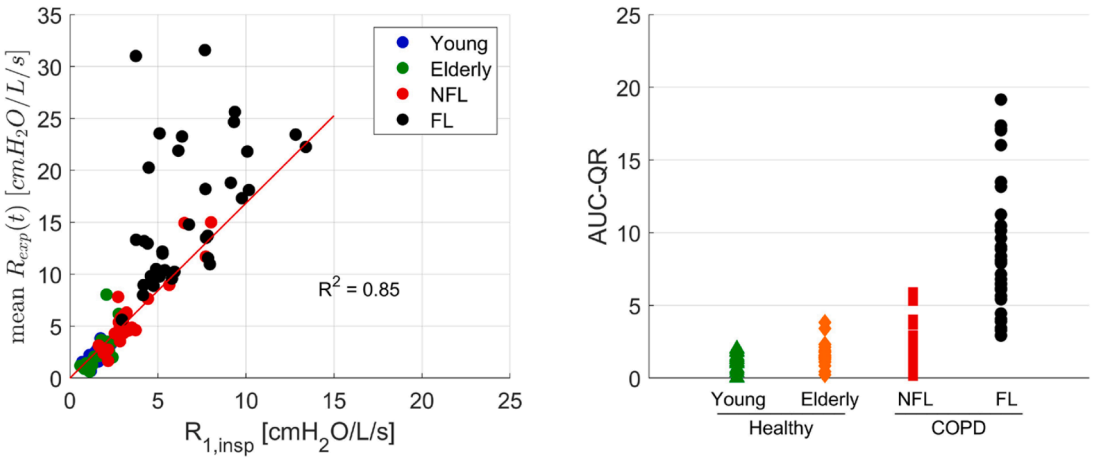

Fig. 4. (left) Correlation of inspiratory and expiratory resistance around the 1:1 line. (right) Distributions of the area under the expiratory resistance-flow curve (AUC-RQ) for all four cohorts.

pressure (Eq. 2). By contrast, variance of expiratory AUC-PV was not well explained by inspiratory AUC-PV ($R_2 = 0.25$)) Similarly, Fig. 4 shows deviation from the tight linear correlation between inspiratory resistance and mean expiatory resistance in FL COPD patients. In Fig. 4, of patients with COPD, only those with FL move away from the line of best fit, suggesting NFL patients have some consistency in underlying mechanistic dynamics contributing to overall increased resistance between inspiration and expiration, and may thus capture an intermediate condition.

Hence, overall, the results presented support the model-based $R_{2,exp}(t)$ term in its ability to capture the nonlinear dynamics of expiratory resistance in Figs. 1, 2 and Tables 1, 2. The results in Figs. 3 **and** 4 show good discrimination of FL versus NFL and healthy subjects, but only moderate discrimination with no p-value for discriminating the evolution of NFL to FL patients. In all cases, flow limitations were assessed using NEP, but the results found track well with the FVC results for each cohort in Table 1 with FVC decreasing with age, COPD, and flow limitation. There is thus consistency between the model-based results and the clinical data for discriminating between FL and healthy subjects. However, the discrimination of NFL subjects from either FL or healthy cohorts was not clear.

The results presented here build on those of D'Angelo et al [11], who utilise (implicit) linear resistance models of inspiratory and expiratory resistance, and their ratio, to discriminate between healthy and COPD patients. Such an approach exploits the higher average expiratory resistance seen in Fig. 4, which is exacerbated by the sharp rise in resistance at end expiration (Fig. 2). While some ratio of expiratory and inspiratory resistance shows promise in discriminating between healthy and COPD patients in their analysis, the authors note that the 95th percentile confidence interval on their analysis is wide [11,29,39]. The advantage of a nonlinear approach to describing expiratory resistance is that all shape dynamics are captured, providing additional information that may add to clinical diagnoses, giving greater insight to more borderline or complex conditions and better describing disease progression.

One study limitation is NEP cannot be applied within the Plethysmograph, requiring separate procedures [29]. In addition, NEP detects the presence of FL at a set additive pressure gradient, and may miss tEFL under higher pressure gradients, or diagnose tEFL is not significantly present under the breathing conditions and methodology for Plethysmography. These issues may explain why some FL subjects have resistance values falling close to the line of best fit in Fig. 4, as it is possible they were not as significantly flow limited during the Plethesmographic breathing recording. Alternatively, deviation from this line of best fit may indicate some specific underlying mechanism, such as airway collapse, which could be investigated in future work. Prospective future studies should also explore the different underlying COPD conditions and their effects on expiratory R dynamics, as modelled here.

A limitation of using plethysmographic data includes the assumptions made to calculate alveolar pressure from shift volume with the application of the ideal gas law, but are mitigated by the specific manoeuvres and/or clinical conditions used during plethysmography [27]. The alveolar pressure surrogate derived from plethysmographic measurements represents an average alveolar pressure across the entire lung, rather than a anatomically specific measurable pressure. However, the assumptions inherent in this derived alveolar pressure match the underlying assumptions of a single compartment lung model, as used here.

A limitation of the single compartment model is the inability to capture heterogeneity. Lung geometry differs for each side of the lung even in normal healthy people, and heterogeneity in underlying lung mechanics and disease progression may mask some clinical disease manifestations in plethysmographic data. However, Plethysmography is a widely-used and well understood analysis tool, and this analysis aims to improve its utility by providing extra model-based insight from the existing data it provides.

The nonlinear model-based airway resistance and resulting metrics presented here, may be of clinical utility in the diagnosis and monitoring of COPD conditions using Plethysmography alone. Use of NEP requires additional procedures and clinical expertise for result interpretation [26, 29]. Other tEFL detection methods are summarised elsewhere [26], but require specific breathing manoeuvres, and therefore patient co-operation, or specialist technology. Thus, a method to suggest or detect the presence of tEFL during standard Plethysmographic measurements has the potential to improve clinical diagnosis and monitoring of COPD conditions, without adding clinical or patient burden.

Table 3
Identified model parameters for each patient, with an identifier for the 4 cohorts, old (O), young (Y), non-flow limited COPD (NFL), and flow limited COPD (FL), with inspiratory resistance ($R_{1,insp}$), expiratory resistance ($R_{1,exp}$), mean $R_{2,exp}(t)$, root mean squared error for the linear model, and root mean squared error for the nonlinear model per subject. Table 3a: subjects 1–40, Table 3b: subjects 41–80, Table 3c: subjects 81–100.

Patient	Category	$R_{1,insp}$	$R_{1,exp}$	Linear RMSE	Mean_$R_{2,exp}$(t)	Nonlinear RMSE
1	Y	1.6	3.0	0.6	2.9	0.2
2	Y	1.7	3.5	0.5	3.8	0.1
3	Y	1.5	2.6	0.4	2.5	0.1
4	Y	2.3	3.0	0.3	3.3	0.1
5	Y	1.1	1.2	0.2	1.0	0.1
6	Y	1.2	1.0	0.2	0.7	0.1
7	Y	1.1	2.0	0.3	2.2	0.1
8	Y	1.1	1.6	0.2	1.2	0.0
9	Y	0.9	1.7	0.3	1.6	0.1
10	Y	1.6	1.6	0.3	1.6	0.2
11	Y	1.2	1.3	0.2	2.0	0.1
12	Y	1.0	1.8	0.2	1.7	0.1
13	Y	1.5	1.7	0.3	1.6	0.1
14	Y	0.7	1.5	0.2	1.5	0.1
15	Y	1.9	3.1	0.4	3.6	0.1
16	Y	1.6	2.3	0.2	2.7	0.1
17	Y	1.4	1.6	0.3	1.9	0.2
18	Y	1.2	2.1	0.3	2.1	0.1
19	Y	1.1	1.5	0.2	1.5	0.1
20	Y	1.8	3.0	0.3	3.0	0.1
21	Eld	2.8	2.7	0.4	6.2	0.2
22	Eld	1.8	2.6	0.3	2.6	0.1
23	Eld	2.4	2.9	0.6	3.5	0.2
24	Eld	2.3	2.9	0.3	3.5	0.1
25	Eld	0.8	0.7	0.2	0.9	0.1
26	Eld	1.6	1.9	0.3	2.1	0.1
27	Eld	1.8	3.4	0.4	3.7	0.2
28	Eld	2.2	2.7	0.3	2.6	0.1
29	Eld	1.3	1.1	0.2	1.3	0.1
30	Eld	2.1	3.1	0.6	3.0	0.1
31	Eld	2.4	1.7	0.3	2.0	0.1
32	Eld	2.1	4.6	0.5	8.0	0.1
33	Eld	2.1	3.0	0.3	3.1	0.1
34	Eld	0.9	1.5	0.3	1.4	0.1
35	Eld	1.1	0.4	0.3	0.6	0.2
36	Eld	1.7	2.1	0.2	2.2	0.1
37	Eld	1.4	1.8	0.3	2.1	0.1
38	Eld	1.1	1.5	0.2	1.5	0.1
39	Eld	0.6	1.2	0.2	1.2	0.1
40	Eld	2.1	2.8	0.4	3.5	0.1
41	NFL	2.8	4.8	0.5	5.4	0.1
42	NFL	7.7	11.8	1.2	11.7	0.4
43	NFL	2.8	4.0	0.5	4.1	0.1
44	NFL	1.7	3.1	0.5	3.0	0.2
45	NFL	3.0	4.0	0.4	4.3	0.1
46	NFL	3.1	6.1	0.7	6.1	0.1
47	NFL	3.5	5.1	0.4	4.9	0.1
48	NFL	8.0	15.2	2.2	15.0	0.4
49	NFL	1.9	2.0	0.3	2.4	0.1
50	NFL	2.8	3.6	0.3	3.5	0.1
51	NFL	2.9	5.2	0.7	5.8	0.1
52	NFL	4.4	7.1	1.0	7.6	0.2
53	NFL	6.5	15.1	2.4	14.9	0.4
54	NFL	3.2	6.4	0.9	6.3	0.1
55	NFL	3.7	3.7	0.9	4.6	0.3
56	NFL	5.6	8.7	1.0	9.0	0.2
57	NFL	2.6	3.9	0.6	4.3	0.1
58	NFL	2.2	2.8	0.4	2.8	0.1
59	NFL	2.2	1.6	0.4	1.7	0.1
60	NFL	3.0	3.9	0.4	5.3	0.1
61	NFL	3.2	4.2	0.4	4.9	0.1
62	NFL	2.7	7.8	1.3	7.8	0.2
63	NFL	3.3	4.0	0.6	4.6	0.1
64	NFL	2.8	4.6	0.8	4.9	0.2
65	NFL	1.6	2.9	0.4	3.1	0.1
66	FL	7.8	12.9	1.5	13.7	0.3
67	FL	6.2	12.5	2.7	21.9	0.2
68	FL	5.1	8.7	1.8	9.8	0.3
69	FL	5.8	8.3	1.3	9.6	0.3
70	FL	4.4	11.0	1.7	13.0	0.1
71	FL	13.4	19.0	3.3	22.3	0.8
72	FL	9.4	18.2	2.6	25.6	0.4

(*continued on next page*)

Table 3 (*continued*)

Patient	Category	$R_{1,insp}$	$R_{1,exp}$	Linear RMSE	Mean_$R_{2,exp}$(t)	Nonlinear RMSE
73	FL	7.7	16.7	3.6	31.6	0.3
74	FL	3.7	12.0	3.8	31.0	0.2
75	FL	9.1	13.7	3.3	18.8	0.6
76	FL	4.2	7.3	1.2	8.0	0.1
77	FL	9.3	22.6	3.5	24.7	0.5
78	FL	4.5	13.1	3.3	20.3	0.3
79	FL	4.2	7.4	1.6	9.0	0.2
80	FL	5.4	8.9	1.0	10.4	0.2
81	FL	5.9	10.1	1.5	10.2	0.2
82	FL	4.7	7.0	0.9	8.9	0.2
83	FL	5.3	10.1	1.1	12.0	0.1
84	FL	3.0	5.2	0.7	5.6	0.1
85	FL	12.8	18.8	1.8	23.4	0.4
86	FL	9.8	12.5	1.7	17.3	0.5
87	FL	5.3	11.4	1.4	12.2	0.2
88	FL	6.4	12.3	2.8	23.3	0.3
89	FL	4.2	10.0	2.6	13.2	0.1
90	FL	10.1	18.2	2.0	21.8	0.3
91	FL	6.8	13.5	2.9	14.8	0.4
92	FL	10.2	16.4	1.5	18.1	0.4
93	FL	7.7	8.6	1.3	13.5	0.6
94	FL	3.8	9.5	2.6	13.3	0.2
95	FL	5.1	16.2	5.0	23.6	0.2
96	FL	7.8	8.5	1.1	11.5	0.4
97	FL	4.6	8.5	1.4	9.8	0.2
98	FL	7.7	16.0	2.5	18.2	0.3
99	FL	4.9	7.9	1.3	10.5	0.2
100	FL	8.0	10.3	1.2	11.0	0.4

5. Conclusions

A model-based method is presented which quantifies nonlinear expiratory resistance in healthy and COPD patients, and is compared to the linear model typical of current clinical analyses. A linear resistance term generally described inspiratory airway resistance well, but only described expiratory resistance in healthy cohorts. COPD patients with and without expiratory flow limitation showed nonlinear dynamics in expiratory resistance, which were most significant in the presence of flow limitation. FL COPD patients showed nonlinear dynamics in airway resistance with decelerating expiratory flow, and in particularly had increasing resistance near end-expiration. FL COPD patients are clearly separated from healthy patients when the area under the resistance-flow curve was compared. Overall, this model-based analysis was able to differentiate COPD and healthy patients, and capture disease progression. Thus, a non-linear expiratory resistance derived from plethysmographic data may be a clinically useful tool in the diagnosis and monitoring of COPD progression.

Funding

This work was supported by the NZ MedTech Centre of Research Excellence (MedTech CoRE, # 3705718).

CRediT authorship contribution statement

Theodore Lerios: Writing – review & editing, Writing – original draft, Validation, Software, Methodology, Formal analysis, Conceptualization. **Jennifer L. Knopp:** Writing – review & editing, Writing – original draft, Validation, Software, Methodology, Formal analysis, Conceptualization. **Camilla Zilianti:** Writing – review & editing, Investigation, Data curation. **Matteo Pecchiari:** Writing – review & editing, Writing – original draft, Methodology, Investigation, Formal analysis, Data curation, Conceptualization. **J. Geoffrey Chase:** Writing – review & editing, Writing – original draft, Validation, Supervision, Methodology, Investigation, Funding acquisition, Formal analysis.

Declaration of competing interest

The authors declare the following financial interests/personal relationships which may be considered as potential competing interests: J. Geoffrey Chase reports financial support was provided by New Zealand Tertiary Education Commission. No further activities to disclose If there are other authors, they declare that they have no known competing financial interests or personal relationships that could have appeared to influence the work reported in this paper.

Acknowledgements

The authors wish to gratefully acknowledge the contributions made to collect and collate the data by the Pecchiari et al. research group.

Appendix A

Fig. 5

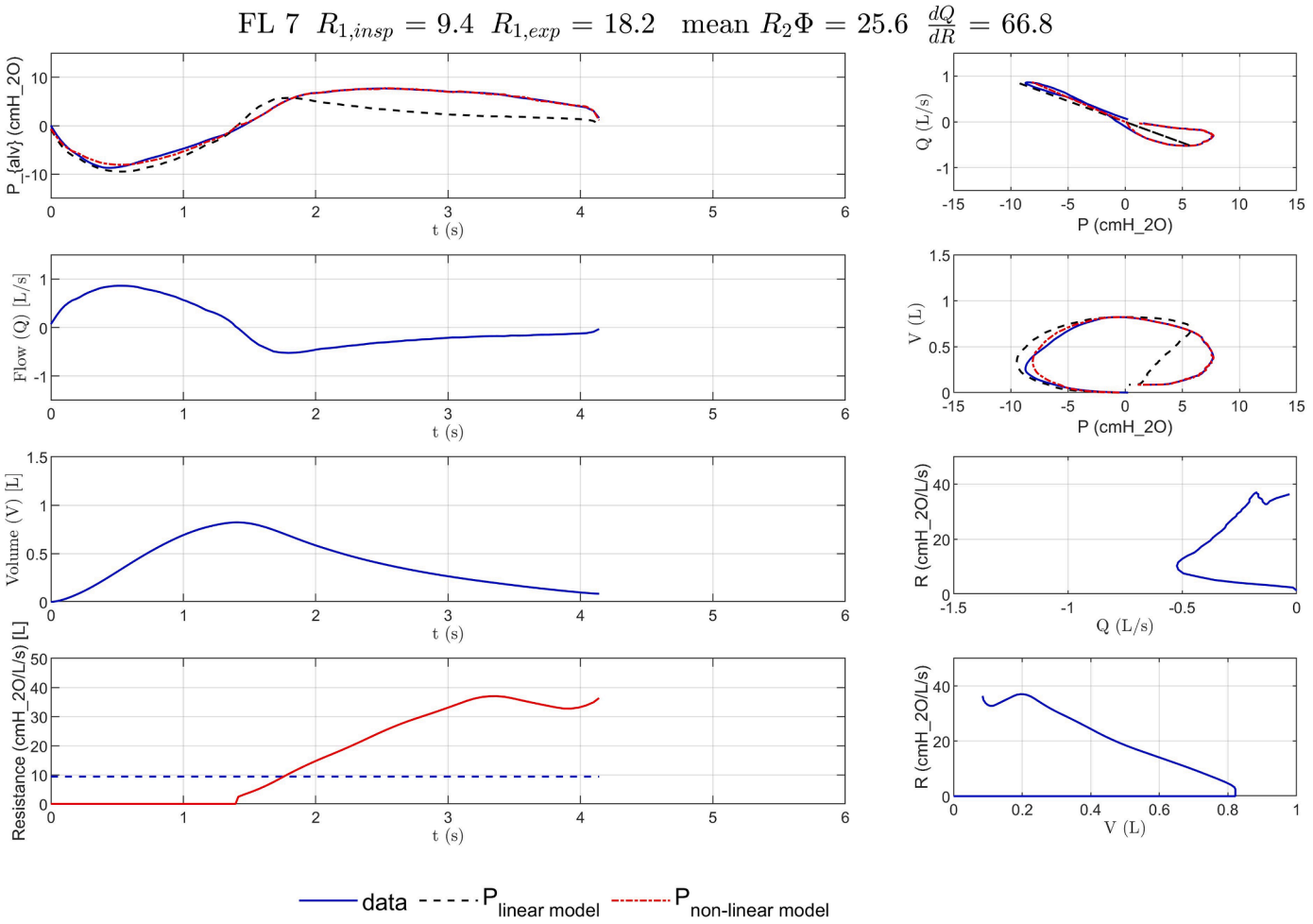

Fig. 5. An example of a patient's plethysmographic alveolar pressure (P_{alv}) data as a function of time, plotted against the linear (black dotted line) and nonlinear (red dotted line) models of alveolar pressure. Flow (Q) as a function of time, volume (V) as a function of time, resistance (R) as a function of time with the linear model constant resistance (blue dotted line), and the nonlinear model dynamic resistance term, $R_2\Phi$ (red dotted line), a pressure-flow loop with model comparisons, a pressure-volume loop, resistance as a function of flow, and resistance as a function of volume.

References

[1] C.F. Vogelmeier, G.J. Criner, F.J. Martinez, A. Anzueto, P.J. Barnes, J. Bourbeau, B. R. Celli, R. Chen, M. Decramer, L.M. Fabbri, et al., Global strategy for the diagnosis, management, and prevention of chronic obstructive lung disease 2017 report. gold executive summary, Am. J. Respir. Crit. Care Med. 195 (5) (2017) 557–582.

[2] J.-L. Vincent, E. Abraham, P. Kochanek, F.A. Moore, M.P. Fink, Textbook of Critical Care E-Book, Elsevier Health Sciences, 2011.

[3] A. Khakban, D.D. Sin, J.M. FitzGerald, B.M. McManus, R. Ng, Z. Hollander, M. Sadatsafavi, The projected epidemic of chronic obstructive pulmonary disease hospitalizations over the next 15 years. a population-based perspective, Am. J. Respir. Crit. Care Med. 195 (3) (2017) 287–291.

[4] P.J. Barnes, Chronic obstructive pulmonary disease: a growing but neglected global epidemic, PLoS Med. 4 (5) (2007) e112.

[5] G. Viegi, S. Maio, S. Fasola, S. Baldacci, Global burden of chronic respiratory diseases, J. Aerosol Med. Pulmonary Drug Delivery 33 (4) (2020) 171–177.

[6] C. Lin, M. Martins, S. Farhat, C. Pope 3rd, G. Conceic¸ao, V. Anastácio, M. Hatanaka, W. Andrade, W. Hamaue, G. Bo̊hm, et al., Air pollution and respiratory illness of children in såo paulo, brazil, Paediatr. Perinat. Epidemiol. 13 (4) (1999) 475–488.

[7] K. Crothers, A.A. Butt, C.L. Gibert, M.C. Rodriguez-Barradas, S. Crystal, A. C. Justice, et al., Increased copd among hiv-positive compared to hiv-negative veterans, Chest 130 (5) (2006) 1326–1333.

[8] I. Bergdahl, K. Toren, K. Eriksson, U. Hedlund, T. Nilsson, R. Flodin, B. Järvholm, Increased mortality in copd among construction workers exposed to inorganic dust, Eur. Respir. J. 23 (3) (2004) 402–406.

[9] C.A. Vaz Fragoso, G. McAvay, P.H. Van Ness, R. Casaburi, R.L. Jensen, N. MacIntyre, H.K. Yaggi, T.M. Gill, J. Concato, Phenotype of spirometric impairment in an aging population, Am. J. Respir. Crit. Care Med. 193 (7) (2016) 727–735.

[10] B. Mahut, A. Caumont-Prim, L. Plantier, K. Gillet-Juvin, E. Callens, O. Sanchez, B. ChevalierBidaud, P. Bokov, C. Delclaux, Relationships between respiratory and airway resistances and activity-related dyspnea in patients with chronic obstructive pulmonary disease, Int. J. Chronic Obstructive Pulmonary Disease 7 (2012) 165.

[11] E. D'Angelo, D. Radovanovic, P. Barbini, P. Santus, M. Pecchiari, Plethysmographic assessment of tidal expiratory flow limitation, Respir. Physiol. Neurobiol. 296 (2022) 103801.

[12] R. Dellaca, P. Santus, A. Aliverti, N. Stevenson, S. Centanni, P. Macklem, A. Pedotti, P. Calverley, Detection of expiratory flow limitation in copd using the forced oscillation technique, Eur. Respir. J. 23 (2) (2004) 232–240.

[13] O. Diaz, C. Villafranca, H. Ghezzo, G. Borzone, A. Leiva, J. Milic-Emil, C. Lisboa, Role of inspiratory capacity on exercise tolerance in copd patients with and without tidal expiratory flow limitation at rest, Eur. Respir. J. 16 (2) (2000) 269–275.

[14] N.G. Koulouris, I. Dimopoulou, P. Valta, R. Finkelstein, M.G. Cosio, J. Milic-Emili, Detection of expiratory flow limitation during exercise in copd patients, J. Appl. Physiol. 82 (3) (1997) 723–731.

[15] C. Tantucci, C. Corbeil, M. Chasse, F. Robatto, S. Nava, J. Braidy, N. Matar, J. Milic-Emili, Flow and volume dependence of respiratory system flow resistance in patients with adult respiratory distress syndrome, Am. Rev. Respir. Dis. 145 (2 Pt 1) (1992) 355–360.

[16] F.M. Franssen, R. Broekhuizen, P.P. Janssen, E.F. Wouters, A.M. Schols, Limb muscle dysfunction in copd: effects of muscle wasting and exercise training, Med. Sci. Sports Exercise 37 (1) (2005) 2–9.

[17] N. Koulouris, P. Valta, A. Lavoie, C. Corbeil, M. Chassé, J. Braidy, J. Milic-Emili, A simple method to detect expiratory flow limitation during spontaneous breathing, Eur. Respir. J. 8 (2) (1995) 306–313.

[18] C. Tantucci, Expiratory flow limitation definition, mechanisms, methods, and significance, Pulmonary Medicine 2013 (2013).

[19] H.A. Van Helvoort, Y.F. Heijdra, H.M. Thijs, J. Viña, G.J. Wanten, P.R. Dekhuijzen, et al., Exercise-induced systemic effects in muscle-wasted patients with copd, Med. Sci. Sports Exerc. 38 (9) (2006) 1543.
[20] E.P. Theodorakopoulou, S.-A. Gennimata, M. Harikiopoulou, G. Kaltsakas, A. Palamidas, A. Koutsoukou, C. Roussos, E.N. Kosmas, P. Bakakos, N.G. Koulouris, Effect of pulmonary rehabilitation on tidal expiratory flow limitation at rest and during exercise in copd patients, Respir. Physiol. Neurobiol. 238 (2017) 47–54.
[21] R.L. Dellaca`, P.P. Pompilio, P. Walker, N. Duffy, A. Pedotti, P.M. Calverley, Effect of bronchodilation on expiratory flow limitation and resting lung mechanics in copd, Eur. Respir. J. 33 (6) (2009) 1329–1337.
[22] E. Boni, L. Corda, D. Franchini, P. Chiroli, G. Damiani, L. Pini, V. Grassi, C. Tantucci, Volume effect and exertional dyspnoea after bronchodilator in patients with copd with and without expiratory flow limitation at rest, Thorax 57 (6) (2002) 528–532.
[23] D.E. O'Donnell, Assessment of bronchodilator efficacy in symptomatic copd: is spirometry useful? Chest 117 (2) (2000) 42S–47S.
[24] P. Calverley, N. Koulouris, Flow limitation and dynamic hyperinflation: key concepts in modern respiratory physiology, Eur. Respir. J. 25 (1) (2005) 186–199.
[25] R.L. Dellaca`, N. Duffy, P.P. Pompilio, A. Aliverti, N.G. Koulouris, A. Pedotti, P. M. Calverley, Expiratory flow limitation detected by forced oscillation and negative expiratory pressure, Eur. Respir. J. 29 (2) (2007) 363–374.
[26] N. Koulouris, G. Hardavella, Physiological techniques for detecting expiratory flow limitation during tidal breathing, European Respiratory Review 20 (121) (2011) 147–155.
[27] C. Criée, S. Sorichter, H. Smith, P. Kardos, R. Merget, D. Heise, D. Berdel, D. Köhler, H. Magnussen, W. Marek, et al., Body plethysmography–its principles and clinical use, Respir. Med. 105 (7) (2011) 959–971.
[28] M.R. Miller, J. Hankinson, V. Brusasco, F. Burgos, R. Casaburi, A. Coates, R. Crapo, P. Enright, C. Van Der Grinten, P. Gustafsson, et al., Standardisation of spirometry, Eur. Respir. J. 26 (2) (2005) 319–338.
[29] M. Pecchiari, D. Radovanovic, C. Zilianti, L. Saderi, G. Sotgiu, E. D'Angelo, P. Santus, Tidal expiratory flow limitation induces expiratory looping of the alveolar pressure-flow relation in copd patients, J. Appl. Physiol. 129 (1) (2020) 75–83.
[30] Q. Sun, C. Zhou, J.G. Chase, Parameter updating of a patient-specific lung mechanics model for optimising mechanical ventilation, Biomed. Signal Process. Control 60 (2020) 102003.
[31] J.G. Chase, J.-C. Preiser, J.L. Dickson, A. Pironet, Y.S. Chiew, C.G. Pretty, G. M. Shaw, B. Benyo, K. Moeller, S. Safaei, et al., Next-generation, personalised, model-based critical care medicine: a stateof-the art review of in silico virtual patient models, methods, and cohorts, and how to validation them, Biomed. Eng. Online 17 (1) (2018) 1–29.
[32] J.L. Knopp, J.G. Chase, K.T. Kim, G.M. Shaw, Model-based estimation of negative inspiratory driving pressure in patients receiving invasive nava mechanical ventilation, Comput. Methods Programs Biomed. 208 (2021) 106300.
[33] E.F.S. Guy, J.G. Chase, J.L. Knopp, G.M. Shaw, Quantifying ventilator unloading in CPAP ventilation, Comput. Biol. Med. 142 (2022) 105225.
[34] Y.S. Chiew, "Model-based mechanical ventilation for the critically ill," 2013.
[35] K.T. Kim, J. Knopp, B. Dixon, G. Chase, Quantifying neonatal pulmonary mechanics in mechanical ventilation, Biomed. Signal Process. Control 52 (2019) 206–217.
[36] D. Radovanovic, M. Pecchiari, F. Pirracchio, C. Zilianti, E. D'Angelo, P. Santus, Plethysmographic Loops: A Window on the Lung Pathophysiology of COPD Patients, Frontiers in Physiology 9 (2018) 484.
[37] C. Zilianti, P. Santus, M. Pecchiari, E. D'Angelo, D. Radovanovic, Diagnostic insights from plethysmographic alveolar pressure assessed during spontaneous breathing in copd patients, Diagnostics 11 (6) (2021) 918.
[38] Y. Yamauchi, T. Kohyama, T. Jo, T. Nagase, Dynamic change in respiratory resistance during inspiratory and expiratory phases of tidal breathing in patients with chronic obstructive pulmonary disease, Int. J. Chronic Obstructive Pulmonary Disease 7 (2012) 259.
[39] M. Pecchiari, D. Radovanovic, P. Santus, E. D'Angelo, Airway occlusion assessed by single breath n2 test and lung pv curve in healthy subjects and copd patients, Respir. Physiol. Neurobiol. 234 (2016) 60–68.
[40] P. Paredi, M. Goldman, A. Alamen, P. Ausin, O.S. Usmani, N.B. Pride, P.J. Barnes, Comparison of inspiratory and expiratory resistance and reactance in patients with asthma and chronic obstructive pulmonary disease, Thorax 65 (3) (2010) 263–267.
[41] A. Nasr, L. Jarenbäck, L. Bjermer, and E. Tufvesson, "Assessment of expiratory vs inspiratory resistance and reactance using fot as a measure of air trapping," 2019.
[42] P. Docherty, T. Lerios, B. Laufer, K. Moeller, and G. Chase, "A method for observing ongoing patient respiratory behaviour with the narx model," 2020.
[43] T. Lerios, J.L. Knopp, L. Holder-Pearson, E.F. Guy, J.G. Chase, An identifiable model of lung mechanics to diagnose and monitor copd, Comput. Biol. Med. 152 (2023) 106430.
[44] J.L. Knopp, E. Guy, K.T. Kim, G.M. Shaw, J.G. Chase, B-spline modelling of inspiratory drive in nava-ventilated patients, IFAC-PapersOnLine 54 (15) (2021) 103–108.
[45] R. Langdon, P.D. Docherty, Y.-S. Chiew, K. Moeller, J.G. Chase, Use of basis functions within a non-linear autoregressive model of pulmonary mechanics, Biomed. Signal Process. Control 27 (2016) 44–50.
[46] C. Guerin, M. Coussa, N. Eissa, C. Corbeil, M. Chasse, J. Braidy, N. Matar, J. Milic-Emili, Lung and chest wall mechanics in mechanically ventilated copd patients, J. Appl. Physiol. 74 (4) (1993) 1570–1580.
[47] C. Tantucci, C. Corbeil, M. Chasse, J. Braidy, N. Matar, J. Milic-Emili, Flow resistance in patients with chronic obstructive pulmonary disease in acute respiratory failure, Am. Rev. Respir. Dis. 144 (1991) 384–389.
[48] R. Peslin, R. Farre, M. Rotger, D. Navajas, Effect of expiratory flow limitation on respiratory mechanical impedance: a model study, J. Appl. Physiol. 81 (6) (1996) 2399–2406.
[49] C. Zhou, J.G. Chase, Q. Sun, J. Knopp, M.H. Tawhai, T. Desaive, K. Möller, G. M. Shaw, Y.S. Chiew, B. Benyo, Reconstructing asynchrony for mechanical ventilation using a hysteresis loop virtual patient model, BioMedical Engineering OnLine 21 (1) (2022) 1–20.
[50] S.E. Morton, J.L. Knopp, M.H. Tawhai, P. Docherty, K. Moeller, S.J. Heines, D. C. Bergmans, J.G. Chase, Virtual patient modeling and prediction validation for pressure controlled mechanical ventilation, IFAC-PapersOnLine 53 (2) (2020) 16221–16226.